N-acetylcholinesterase-induced apoptosis in Alzheimer's disease.

Download Here

ADVERTISEMENT

Morpholino Oligos

GENE

www.

OPEN ACCESS PEER-REVIEWED

RESEARCH ARTICLE

N-Acetylcholinesterase-Induced Apoptosis in Alzheir Disease

Debra Toiber, Amit Berson, David Greenberg, Naomi Melamed-Book, Sophia Diamant, Hermona Sor

Published: September 1, 2008 • https://doi.org/10.1371/journal.pone.0003108

Figures

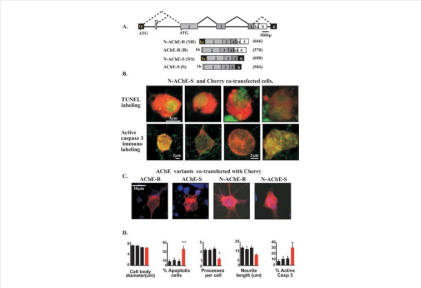

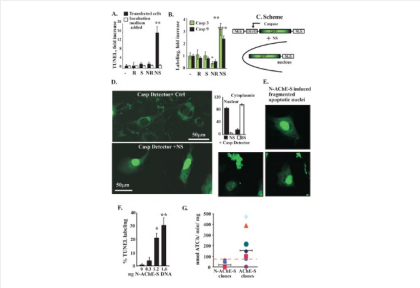

Abstract

Background

Alzheimer's disease (AD) involves loss of cholinergic neurons and T
phosphorylation. Here, we report that overexpression of an N-termi
“synaptic” acetylcholinesterase variant, N-AChE-S is causally involv
phenomena.

Methodology and Principal Findings

In transfected primary brain cultures, N-AChE-S induced cell death,
impairments and caspase 3 activation. Rapid internalization of fluor
fasciculin-2 to N-AChE-S transfected cells indicated membranal loca
lines, N-AChE-S transfection activated the Tau kinase GSK3, induced
phosphorylation and caused apoptosis. N-AChE-S-induced cell dea
inhibiting GSK3 or caspases, by enforced overexpression of the an
proteins, or by AChE inhibition or silencing. Moreover, inherent N-AC
by stressors inducing protein misfolding and calcium imbalances, b
AD; and in cortical tissues from AD patients, N-AChE-S overexpressi
hyper-phosphorylation.

Conclusions

Together, these findings attribute an apoptogenic role to N-AChE-S
value to AChE inhibitor therapeutics in early AD.

Citation: Toiber D, Berson A, Greenberg D, Melamed-Book N, Dia
(2008) N-Acetylcholinesterase-Induced Apoptosis in Alzheimer's
3(9): e3108. https://doi.org/10.1371/journal.pone.0003108

Editor: Joseph Najbauer, City of Hope Medical Center, United Sta

Received: April 2, 2008; **Accepted:** August 8, 2008; **Published:** Se

Copyright: © 2008 Toiber et al. This is an open-access article di
terms of the Creative Commons Attribution License, which permi
distribution, and reproduction in any medium, provided the origi
source are credited.

Funding: This research was supported by the European Union's
Excellence (LSH-2004-1.1.5-3) and STREP (LSHG-CT-2006-037277
Ministry of Science and German-Israel Project, DIP-G 3.2, the Isra
Science, the Interdisciplinary Center for Neuronal Computation (
ROSETREES Foundation, UK.

Competing interests: The authors have declared that no compe

Introduction

In Alzheimer's disease (AD), premature death of cholinergic neuron
accumulation of neurofibrillary tangles, constituting of hyper-phosp
cholinergic hypothesis attributes the cognitive impairments in AD to
functions [2]. Accordingly, acetylcholinesterase (AChE) inhibitors se
symptoms by prolonging acetylcholine (ACh) availability [3]. Some a
the disease process under treatment with AChE inhibitors [4], [5]; ot
alternative AD therapeutics, including inhibitors of the Tau kinase, G
Kinase 3 (GSK3) [6], [7], or of other key proteins of the apoptotic pat
unclear if these different approaches reflect a single targeted casc
triggers this cascade.

Apoptotic cell death leads to cortical shrinkage in AD brains, accom
loss of cholinergic neurons, which express considerably more AChE
types [8]. Recent reports demonstrated AChE accumulation in apop
inhibition and general silencing were found to prevent apoptosome
death [9], [10]. Such cell death may occur through activation of the
(ER), mitochondrial stress and/or cell surface death receptors [11],
reports raised a new question: how do AChE-expressing neurons s
AChE is not one but several variants, induced by alternate promote
splicing [13]. It occurred to us that some, but not all, AChE variants, r
neuronal cell death which occurs in AD. To challenge this theory, we
expression in the AD cortex, tested the effects of aberrant AChE ge
cultured cells, explored the molecular mechanism(s) involved by ma
and key apoptotic proteins, and searched for pharmacological mea
mitigating the observed apoptotic effects.

Results

N-AChE-S expression induces caspase-mediated cell dea

Overexpression of two short (AChE-S, AChE-R) and two N-terminally
variants(N-AChE-S, N-AChE-R) [13] (Fig 1A), was induced by transient
primary cortical cells, HEK 293 embryonic kidney cells, U87MG gliob
epithel and CHO hamster ovary cells. In primary cortical cells expre
invariably caused apoptosis, observed as increased TUNEL labelin
activation (Fig 1B and C, respectively). Surviving cortical cells transf
showed similar cell body size to those expressing the other variant
extended fewer and shorter processes from the cell body than cell
other variants, indicating ill health for transfected surviving cells (Fig
other tested AChE variant exerted such effects (Fig 1E and Table S1
possibility of indirect effects of secreted AChE or other proteins, by

pre-conditioned medium, removed 24 hr after transfection and add
cells, caused no apoptotic effect (Fig 2A and Table S1). Together, th
caused cell death to intracellular overexpression of N-AChE-S. More
overexpressing cells showed concurrent increases in both activate
2B) and the caspase inhibitor Z-VAD-FMK prevented the N-AChE-S in
below), suggesting a caspase-mediated apoptotic cascade [14]. Hi
specificity of the N-AChE-S-induced effects, caspase 3 levels were i
AChE-R-transfected cells (Fig 2B).Therefore, the N-terminal extensio
be insufficient to cause the cell death conferred by N-AChE-S.

Download:

PPT Pow

PNG larg

TIFF orig

Figure 1. N-AChE-S induced apoptosis in primary cortical cells.
A. AChE mRNA transcripts. Upper scheme: The AChE gene structu
codons are indicated. Lower scheme: corresponding transcripts
open reading frames noted (amino acids). B. Primary cortical cel
micrographs: N-AChE-S and Cherry cells co-transfected with (red
labeled (green). Lower micrographs: Red labeling as above, gre
active caspase-3. C. Effects of AChE variants. Primary cortical ce
transfection with Cherry and different AChE variants co-transfec
show non apoptotic cells with different characteristics. N-AChE-S
confers shrunk features. D. Shown are cell body diameters, perc
cortical cells, No. of ramifications extended from cell bodies, ave
length, and percent of cells labeled with caspase 3 activated an
transfected with (from left to right) AChE-R, AChE-S, N-AChE-R and
columns). Note N-AChE-S induced changes(*p=0.001,**p=0.000
https://doi.org/10.1371/journal.pone.0003108.g001

Download:

PPT Pow

PNG larg

TIFF orig

Figure 2. N-AChE-S induces caspase-mediated cell death.
A. N-AChE-S mediated apoptosis. TUNEL analysis 24 hr post-trans
cells transfected with AChE variants or an “empty” plasmid, comp
transfected cells incubated with pre-conditioned medium (*p=0.

test). B. Caspase immunostaining. N-AChE-S-associated increase
caspase 3 and 9 and N-AChE-R-associated reduction in caspase
(*p=0.04, **p=0.004, ***p=0.0003 Student's t test). C. Caspase
N-AChE-S was co-injected with GFP-NLS vector equipped with NE
caspase-cleavable DEVD motif. Caspase activation yields nuclea
translocation. D. Microinjection-induced caspase-mediated cell
3T3 cells co-injected with an "empty" plasmid and GFP-NES/NLS (
showed cytoplasmic GFP, whereas N-AChE-S co-injected cells (b
showed nuclear fluorescence (columns). Shown are representa
70, $p<10^{-7}$ Student's t test. E. Within 24 hr from injection, cells ex
acquired nuclei with condensed chromatin. F. N-AChE-S-inducible
dependent. Percent of apoptotic U87MG cells under transient tr
increasing plasmid doses. (*p=0.03, **p=0.002 Student's t test).
transfection on cell viability. CHO cells were co-transfected with
AChE-S vectors, and the G-418 antibiotic resistance plasmid, and
days in the presence of G-418. Individual surviving clones were
expanded and cellular AChE activity was measured (p=0.02, Stu
that individual clones transfected with N-AChE-S all showed cons
activity, largely below the average activity in human brain extrac
https://doi.org/10.1371/journal.pone.0003108.g002

To directly estimate the efficiency and dynamics of the N-AChE-S-ind
selected 3T3 cells for microinjecting N-AChE-S. Co-injection of a clea
activated GFP reporter, equipped with a nuclear localization signal
translocation to the nucleus in the presence of activated caspases
served for follow-up of the induced changes. The caspase reporter
were microinjected for control (Fig 2D,E). Within 24 hrs, injection of th
alone induced cytoplasmic GFP fluorescence in 94±3% of the cells (
85±3% of the N-AChE-S injected cells showed nuclear GFP fluoresce
caspase activation, and acquired condensed nuclei characteristic

In cells transiently transfected with >1.2 ng/cell of the N-AChE-S DNA
dose-dependent apoptosis (Fig 2F). Next, individual clones of CHO c
express any endogenous AChE variant were stably transfected with
shorter AChE-S, for comparison. Cloned cells presented considerab
protein than clones stably transfected with AChE-S (also called "taile
reflected in considerably lower ACh hydrolytic activity than that of c
with AChE-S (10±8.4 vs. 150±45 nmol substrate hydrolyzed/min/mg
dashed line). Such low activities, lower than the average activity ob
brain, indicated a possible selective pressure against expression o
levels. Thus, microinjection as well as transient and stable transfec
excess N-AChE-S is incompatible with cell viability.

N-AChE-S displays similar catalytic characteristics to ot

Fractionation and activity tests demonstrated that AChE-S and N-AC
within the cells, whereas AChE-R and N-AChE-R both showed a tend

(Fig S1A).Sequence analysis predicted that while the AChE signal pe
by the N-extended terminus, the new N-AChE variants include an ac
Higher expression levels for the shorter variants were observed by
of transiently transfected cells. Enzymatic Activity (with acetyl-thioch
native gels showed matched differences in enzyme activity (Fig S1E
proportional expression and activity of the various AChE proteins. N
enzymatic characteristics (e.g. Km, substrate inhibition) were indisti
S and N-AChE-R as compared with the shorter variants (Fig S1C,D), i
extended variants are correctly folded. Thus, N-AChE-S was found t
lower levels than the shorter variants, but despite this, it was the or
apoptogenic effect.

N-ACHE-S promotes GSK3 activation and Tau hyper-ph

The relatively low levels of N-AChE-S could potentially be due to mis
activating ER stress-induced apoptosis. To test this possibility, we m
the ER stress markers GRP78 and Xbp. Both GRP78 levels and the ra
and unspliced variants of Xbp were similar to those of cells transfec
variants or control cells (Fig S2A,B), suggesting that the observed ap
were not caused by the misfolded protein response or the ACh hyd
AChE-S. Nevertheless, high levels of N-AChE-S could signal the cell c
inducing another kind of cellular stress, compatible with other case
overexpressed protein can lead to cell death, e.g. hIAPP in B cells[1
relevance to the observed apoptosis of the Tau kinase GSK3, which
modulating Bcl proteins including Bax [17], [18] and was implicated
pathology [19]. We tested the potential involvement of GSK3 in N-AC
apoptosis in U87MG cells, which are more readily amenable for tran
neurons. Supporting such involvement, N-AChE-S expression selec
levels of inactive GSK3 carrying phosphorylated serine, whereas to
levels of hyper-activated GSK3■ and ■ with phosphorylated tyrosi
unchanged (Fig 3A). Thus, larger GSK3 fractions were active under
Moreover, N-ACHE-S overexpression induced progressive increase
phosphorylation of Tau in cultured U87MG cells, reaching a 37% inc
transfection ($P<0.05$, Fig 3B). Correspondingly, U87MG cells transfe
showed 25% enhanced immunolabeling of activated Bax (Fig 3C), su
by the GSK3 inhibitor SB316763, known to suppress cell death [18].
reduced the immunolabeling of both activated Bax and hyper-phos
cultured cells by about 20% as compared to N-AChE-S transfected c
(Fig 3D and data not shown). Also, SB316763 largely prevented the
effect, to a similar extent as caspase inhibition, and without affectin
activity (Fig 3D,E).

Download:
PPT Pow

PNG large

TIFF orig

Figure 3. N-AChE-S induces suppressible GSK3-activation, Tau h phosphorylation and Bax activation.
A. Immunoblots. N-AChE-S reduces serine-phosphorylated P-GSI maintaining unchanged total GSK3■ and tyrosine phosophoryla elevating active-Bax. B. Tau hyper-phoshorylation: N-AChE-S, but N-AChE-R induces progressive increases in hyper-phosphorylat Alpha tubulin 4 served as reference. C. N-AChE-S-inducible GSK3 dephosphorylation facilitates Bax activation. Shown are microgr transfected cells with elevated phosphorylated Bax labeling con control (Ctrl) cells. GSK3 inhibition suppresses this labeling. Qua increase in Bax labeling of NS overexpressing cells, preventable (SB316763) treatment (**p=0.00009 Student's t test). D. GSK3 an inhibition suppress N-AChE-S-induced apoptosis. % TUNEL labeli transfected cells. Note that 5 μM SB316763 (GSK3-I) and 80 μM Z (caspase-I) reduced apoptosis. (GSK-I p=0.000013, Casp3-I p=9 test). E. GSK3 and Caspase inhibitors do not affect AChE catalytic proteins suppress N-AChE-S-induced apoptosis: U87MG cells co AChE-S and Bcl-2 (# p=0.00001), BI (*p=0.03), or Bcl-XL (p=0.054 showed variably suppressed TUNEL labeling.
https://doi.org/10.1371/journal.pone.0003108.g003

Bcl proteins mitigate the N-AChE-S induced apoptosis

Since AChE silencing was shown to prevent apoptosome formation AChE-S effect occurs upstream to the mitochondrial membrane per characteristic of apoptosis. Cultured cells were co-transfected with apoptotic protein Bcl-2 or its family members, Bcl-xL and BI. All of the Bax from triggering the permeabilization of mitochondrial membran the N-AChE-S-induced cell death (Fig 3F), compatible with the notion apoptotic pathway.

Cell surface N-AChE-S location

We considered the possibility that in the N-extended AChE variants, signal peptide can be used as transmembranal domain similar to th neuroligin [20]. To address this issue, we labeled Fasciculin-2, an AC impermeable to the cell membrane, with tetramethyl-rodhamine (Fa which do not express endogenous AChE were co-transfected with N 18 hrs and were exposed to Fas2*. Live imaging was performed be and every 5 minutes after its addition. Cells co-transfected with GFP transfected neighbor cells showed vesicular internalization of Fas2 performed the same experiment and fixed cells after 0,5,15 or 30 m disrupted the vesicles; however, red labeling reflecting internalized cytoplasm of cells expressing GFP+N-AChE-S compared to control c

peaked after 5 minutes from Fas2* addition, remained unchanged a
declined after 30 minutes. Our results indicate that N-AChE-S is posi
membrane with the catalytic domain towards the extracellular spac
binding. In addition, we used antibodies specific for the extended N
comparison to antibodies targeted to the core domain to label N-AC
U87MG cells. An "empty" vector served as control (Fig S3A, scheme)
electron microscopy, N-ACHE-S-transfected cells yielded generally s
patterns with the N-specific and core domain antibodies, peaking u
cellular membrane (Fig S3A,B). Apart from the membrane-associate
11% of the gold beads adhered to endocytotic vesicles (identified b
contours [23], compatible with the Fas2* data.

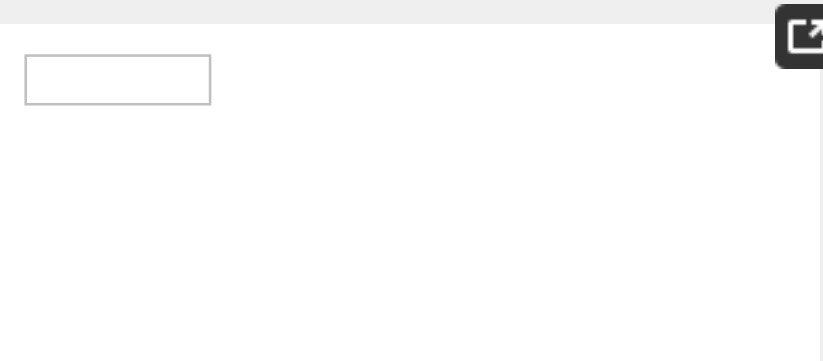

Download:

PPT Pow

PNG larg

TIFF orig

Figure 4. N-AChE-S Membranal localization and Fasciculin-2 Int
A. Fasciculin-2 internalization. Tetramethylrodhamine labeled Fa
added to the medium of 293 cells co-transfected with N-AChE-S a
internalization of labeled Fasciculin 2 yielding fluorescence into
transfected, but not non-transfected cells at 15 and 30 minutes.
taken by live imaging. B. Schematic representation of N-AChE-S i
membrane and its internalization. C. Tetramethylrodhamine labe
add to the medium of N-AChE-S and GFP co-transfected 293 cells
0,5,15 and 30 min. The density of Fasciculin2 was measured. Col
in N-AChE-S transfected vs non-transfected cells at the noted tim
**p>0.005 Student's t test). D. Representative pictures of the ex
in C.1.Merge picture (yellow fluorescence notes Fasciculin2 inte
expressing cells). 2. Co-transfected GFP and N-AChE-S cells. 3. Fa
internalized 4.Light picture.
https://doi.org/10.1371/journal.pone.0003108.g004

Core domain contributions to N-AChE-S-induced apopt

At the extracellular domain of synaptic membranes, neurexin intera
transduce intracellular signals through synaptic protein partners [2
and electron microscopy results, we speculated that the intracellula
AChE-S might similarly mediate intracellular signaling in response to
Given that inhibitor interactions induce structural changes in the AC
we assessed the capacity of the carbamate active site inhibitor, pyr
peripheral site inhibitor of AChE, propidium or the quaternary AChE i
known to be impermeable to the cell membrane [25] to affect N-ACh

apoptosis. All of these agents reduced apoptosis in N-AChE-S-trans
levels observed in N-AChE-R transfected or control cells (Fig 5A). The
demonstrated inherent involvement of the core domain of AChE, wh
embedded, in the N-AChE-S-induced apoptotic process. The simples
mechanism(s) involved therefore suggests that the N-AChE-S-induc
initiate extracellularly, as it is susceptible for suppression by small r
excluded from cellular entrance (e.g. BW284C51) and since such in
prevent the transduction of the signal into the cell.

Download:

PPT Pow

PNG larg

TIFF orig

**Figure 5. N-AChE-S and Thapsigargin induced apoptosis are sup
and siRNA.**

A. Small molecule-mediated suppression of N-AChE-S-induced a
Normalized TUNEL labeling. Inset drawing: Pyridostigmine (Pyr), p
BW284C51 (BW) are variably targeted AChE-Is. Columns: All AChE
death in N-AChE-S but not N-AChE-R-transfected cells (NS vs. NR p
NS+Pyr 0.008, NS vs. NS+BW p=0.000001, NS vs. NS+Pro p=0.00
test) B. Carbachol fails to prevent N-AChE-S-induced cell death. C
did not affect cell death in control, N-AChE-R or N-AChE-S (Blue Sc
empty vector) transfected cells. C. Apoptotic stimuli induce hE1e
QRT-PCR of U87MG cells subjected to the noted agents. Columns
hE1e levels over naive cells (Thapsi *p=0.03, Carb p=0.03, ß-me
n=4). D. AChE-targeted siRNA suppression. AChE targeted siRNA
siRNA reduced AChE activity in cells transfected with either N-AC
(NR ctrl vs NR siRNA p=0.002; NS ctrl vs NS siRNA p=0.002; n=3 di
experiments, Median test). E. siRNA suppression of N-AChE-S-ind
Apoptosis was effectively suppressed in cells co-transfected wi
siRNA, or cells treated with Thapsigargin, but siRNA did not affec
N-AChE-R transfected cells. (NS ctrl vs. NS siRNA p=0.00009, NS v
thapsi ctrl vs. thapsi siRNA p=0.00001, thapsi vs. ctrl p=3^{-7} thaps
siRNA p=0.033, Student's t test). F. The N-AChE-S apoptotic casca
upregulation by apoptotic insults co-activates GSK3 by serine de
facilitating activation of Bax and caspases, yielding apoptosis pr
proteins or GSK3, AChE, and caspase inhibitors.

https://doi.org/10.1371/journal.pone.0003108.g005

Since N-AChE-S is enzymatically active, we further wished to test the
were dying because of the lack of ACh. Addition of the non-degrada
carbachol did not change the observed cell death (Fig 5B), excludin
suggesting structural, rather than enzymatic involvement of the co

induced cell death.

Insult stimuli facilitate inherent N-AChE-S expression a

Notably, various cellular and organismal stimuli induce AChE overex
splicing and alternate promoter choices [13], [26], [27]. Therefore, w
stressors-induced gain of N-AChE-S function on apoptosis outcome
mercaptoethanol, a reducing agent which denatures proteins by re
bonds (0.2 M), or thapsigargin, which releases calcium from the ER a
(10 μM) [28] all induced significant inherent overexpression of the h
the extended N-terminus in U87MG cells (median test p<0.03). In co
NMDA receptor agonist (0.5 mM), and cortisol, a glucocorticoid horm
cells from acute stress responses (0.5 μM) [29] showed no effect on
5C). This called for testing the consequences of loss of N-AChE-S fu
cells co-transfected with N-AChE-S and an AChE-targeted siRNA, los
expression selectively abolished its apoptotic effect. siRNA also am
death induced by thapsigargin; in comparison, suppressed N-AChE
cortisol treatment had no effect (Fig 5D,E). Thus, inherent gain of N-A
induced apoptosis, whereas loss of its function suppressed it. Toge
identified N-AChE-S as an upstream apoptotic trigger encompassing
"classical" cell death elements (Fig 5F) and likely acting through the
unknown intracellular element(s) with the N-terminal extended dom

N-AChE-S expression in AD

Last, but not least, we turned to the AD brain. When protein from co
differentially extracted in detergent and salt-containing solutions, A
showed reduced AChE activity as compared to matched non-deme
Reduction was observed in the membrane-associated fraction (whe
[30]) (Fig 6A). Neither the soluble nor the membrane protein fraction
decreases, indicating that the reduction was primarily of AChE-S, lik
loss of cholinergic neurons. In NDC cortices, quantitative real-time R
each cDNA clone showed that transcripts spanning the hE1e exon
terminal extension represent approximately 6% of total AChE mRNA
ng RNA, compared to 55,700 transcripts of total AChE mRNA per ng)
that both the core domain and the major exon 6 decreased by 40+/
compared with NDC cortical tissues (Fig 6B, and data not shown). Th
contained less AChE-S (which normally constitutes 90% of the enzy
amounts as NDC of N- AChE and AChE-R (each constituting about 6%
transcripts).

Download:
PPT Pow
PNG larg

TIFF orig

Figure 6. N-AChE-S overexpression in AD cortical neurons assoc hyper-phosphorylation.
A. Differential fractionation of AChE hydrolytic activity. Cortical pr fractionated into low salt (LS, soluble protein), low salt detergent associated) and high salt (HS, integral membrane and nuclear p activity was measured. Note decrease in LSD (AChE-S-enriched) or HS fractions (p=0.0476, n=4 NDC, 8AD, Median test). B. AD-ass AChE mRNA transcripts. Columns: QRT-PCR. Note AD-associated compared to NDC samples in the S, but not the N or R encoding e 10 AD, 5 NDC Wilcoxon Two Sample Test). C. Inset is: E1e labeling sections from human entorhinal cortex. Columns are quantificat density per area. (Median test, *p=0.0286, n=4 in each group). D Immunostaining in AD and NDC cortices. Columns are quantifica area (*p=0.029 n=5 NDC, 9AD Median Test). E. AD Entorhinal cor immunolabeled for N-AChE, AChE-S or hyper-phosphorylated Tau AChE-S labeling correlate with Tau-P density. Tau-P, N-AChE, and were quantified using immunohistochemistry on sections from t cortex of AD patients. (Pearson's correlation for N-AChE and Tau
https://doi.org/10.1371/journal.pone.0003108.g006

Our mRNA analyses suggested that in the remaining cholinergic ne constitutes a larger part of AChE than in NDC brains. To challenge th used quantified FISH analysis which indeed identified 273% enhanc AD cortical cells with neuronal morphology as compared with NDC s =0.03) (Fig 6C). Immuno-labeling further demonstrated 152% elevat terminus characteristic of N-AChE-S in AD compared to NDC cortices (Fig 6D), together suggesting AD-associated overexpression of N-A neurons.

Association with hyper-phosphorylated Tau in AD

Tau hyper-phosphorylation is a marker of AD pathology that is direc death. Importantly, N-AChE and AChE-S showed similar patterns of e hyper-phosphorylated Tau in the AD cortices. The majority (72, 70 a cells out of approximately 100 in each group) of cells expressing N- phosphorylated Tau were 7–24 μm in length, compatible with the siz 6E). Moreover, the labeling intensity of N-AChE, and to a somewhat s AChE-S (probably because only part of the AChE-S molecules are N- correlated with that of hyper-phosphorylated Tau (Fig 6F). Together these observations are compatible with the hypothesis that N-AChE AD cortical neurons is causally linked with the apoptotic destiny rep expressing hyper-phosphorylated Tau.

Discussion

Recent reports of AChE association with apoptosis [9], [10] left unex
survival of AChE-expressing cholinergic neurons. Our current findir
unequivocal answer to this question by pointing at N-AChE-S as the
variant. We further demonstrate that N-AChE-S induces cell death o
above a critical threshold. To explore the molecular mechanism(s) u
apoptotic role, and to study its relevance for the AD-induced death
we systematically manipulated N-AChE-S expression in cell culture e
demonstrated that gain of N-AChE-S function invariably induces apo
its function improves survival.

Enforced N-AChE-S overexpression induced apoptosis both in prima
different cell lines of various tissue and organismal origins. This att
conserved and ubiquitous role as a general trigger of apoptosis. In
neuronal loss reaches 30–90% [31] in a manner attributable to the
phosphorylated Tau and neurofibrillary tangles [1]. Circulation ACh
during normal aging [32]; moreover, the ApoE4 genotype [33], muta
and the presence of Aß [35]–[37] all induced upregulation of AChE a
upregulation was also reported as being induced by the apoptotic
well as by damaging light in retinal neurons [39]. Here we report tha
reactions and calcium misregulation, both implicated in AD and in th
death [40], lead to N-AChE-S overexpression. Our current findings t
protein involved in all the above phenomena was likely the N-ACHE-
studies will be required to explore the possible function(s) of N-ACh
and define if it is involved, for example in the programmed cell deat
developing neurons [41].

The N-AChE-S, but not the N-AChE-R or the shorter AChE-S variants i
suggesting that both the N- and the-S termini are required for this p
various AChE inhibitors suppressed the N-AChE-S induced apoptosi
central core domain, where AChE's active site is embedded [42] as
involved as well. The most likely explanation for this multi-domain in
structural, rather than enzymatic features of N-AChE-S protein are i
part of the N-AChE-S variant to the cell membrane and demonstrate
interactions and rapid internalization for this protein, suggesting th
terminus of N-AChE-S protrudes intracellularly, similar to the homolo
neuroligin [20]. Inhibitor interactions were shown by others to exert
the AChE molecule [43], indicating parallel changes in N-AChE-S. Tha
inhibitors attenuate the N-AChE-S-induced apoptotic outcome there
core domain transduces signals to the cell through the cytoplasmic
Together, this implies that N-AChE-S likely operates as a bifunctiona
properties characteristic of both enzymes and ligand-activated rec
the above arguments, these findings may also explain the reported
effects of anticholinesterases [4], [5] and can possibly outline testi
prophylactic agents.

Our current finding of increased N-AChE expression in AD cortices,
their core AChE expression and activity, is compatible with the enha
these tissues. Supporting the notion of causal relationship with this
stress and calcium imbalances have been implicated in GSK3 activa

in the AD brain [12] through hyper-phosphorylated Tau, presenilin, A
N-ACHE-S-induced dephosphorylation of the Ser residue activating
properties corroborates this association. Others reported increase
staining in neurons with Tau hyper-phosphorylation. A recent repor
that Tau hyper-phosphorylation is protective [44]. Our findings did n
between these possibilities but demonstrate apparent association
phosphorylation with the N-AChE-S apoptotic mechanism. We furthe
exposure to apoptotic stressors would likely induce N-AChE-S expre
the cholinergic neurons with higher basal AChE expression, and ca
death. At least part of the currently employed AD therapeutics may
of this overexpression by preventing the N-AChE-S-induced apopto
disease progression [4], [5]. Further delineation of this induction an
for preventing the premature death of cholinergic neurons at earlie
disease would therefore merit special attention.

Materials and Methods

Human brain tissue

Brain tissue from AD patients (n=10) and matched non-demented c
obtained from The Netherlands Brain Bank. Ethical approval and wr
from the donors or the next of kin was obtained in all cases. Neurop
staging of neurofibrillary changes (I–VI) was performed *post morten*

Primary cortical cell culture

Cerebral cortex was separated from the brain of 15th day embryos
and cells plated on poly-L-ornithine coated cover slips in Neurobas
supplement, Glutamax and Penicillin/streptomycin (Invitrogen). Tra
performed with lipofectamine 2000 (Invitrogen).

Plasmids

The N-AChE-R and N-AChE-S plasmids are modifications of CMV-ACh
with the hE1e exon inserted in the HindIII cloning sites. Bax Inhibitor
Science Reagents El Cajon, CA, and the caspase detector was from
CA).

Microinjection

NIH 3T3 cells were microinjected using an Axiovert200M Zeiss micro
a microinjection system, incubated for 24 hours and then viewed. T
1024 BioRad confocal scanhead coupled to a Zeiss Axiovert 135M i
with a 40×/NA=1.3 oil immersion objective. GFP was detected at 488
wavelength and a HQ525±20 filter served for collecting emission.

Statistics Methods

Student's t-test was used in cell culture experiments, where cell nu
enough to assume normal distribution.

Median test is a-parametric test was used for comparing the media
populations that were relatively small, assuming abnormal distribut
samples, maximum 10 e.g. mRNA transcripts, protein densities and
compared to control.

The Wilcoxon test was preferred over the median test when one or
were "off scale". It served for calibrating cDNA transcripts from AD a

Pearson correlation test describing the strength of an association b
used to measure the correlation between N-AChE-S and hyper-phos
aim was to test if *linear* relationship exists between these values of

Image analysis

Immunohistochemistry and In situ hybridization experiments were c
ImageJ 1.33 free software (http://rsb.info.nih.gov/ij/).

1. In the "Analyze tool" we chose Set measurements and selected: I
(which measures the density of the selected pixels divided by the n
quantify staining intensity.

2. We used the "freehand selection" tool to draw a line around a sin
measure and then selected an appropriate measure in the "analyz
analyzed many cells (20–30) in each picture. We selected 2–3 empty
determine the background for each picture, and subtracted it from
observed for the measured cells to normalize light efficiency differe
between different pictures.

3. The total average for a single experiment was composed of 4 diff
Standard deviation values were calculated for these averages, to c
possibility that a specific change was an outlier which occurred out
calculated for the other pictures.

The averages of the different groups were used and are depicted i

4. Data collected from the different cells in each picture was used to
value for that picture. In case of cell culture experiments, 5–8 differe
to assess each treatment and were analyzed as noted before.

5. For Western Blot analysis we used the ImageJ Gel Analyzer option
a rectangular shape for each band in the gel. We captured the grap
as area of the band, which should correlate with the quantity of pro
used the areas measured as reflecting protein quantity. Normalizat
the area by that obtained for tubulin 4 from that sample,, which serv
housekeeping standard.

Supplementary methods

Immunohistochemistry, confocal and electron microscopy, fluoresc
hybridization (FISH), cell cultures, siRNA design and production and
were as described [45] (and/or are all detailed under Supplementa

Real Time PCR, TUNEL Apoptosis assay, immunocytochemistry, prote
described [46] (Text S1, Table S3 antibodies list and Table S4 probe

Supporting Information

Text S1.

Supplementary Materials and Methods.
https://doi.org/10.1371/journal.pone.0003108.s001
(0.05 MB DOC)

Figure S1.

N-AChE-S characteristics. A. Cellular and secreted AChE forms. Hydr
AChE variants in transiently transfected U87MG cell extracts and me
R and N-AChE-R are largely secreted, whereas AChE-S and N-AChE-S
Immunoblot and activity staining. Top: Immunoblot. Note low-level ex
and N-AChE-R compared to the corresponding shorter counterparts
staining in a native gel. Note migration and staining intensity differe
Percentage of maximal acetylthiocholine (ATCh) hydrolytic activity a
substrate concentration. Note indistinguishable Km values (0.33±0.
0.35±0.13, and 0.39±0.17) and similar Hill's coefficients (0.94±0.12, 0
0.87±0.18) for the AChE-R, AChE-S, N-AChE-R and N-AChE-S variants,
Substrate inhibition. All variants showed inhibition under acetylthioc
concentrations >5 mM.
https://doi.org/10.1371/journal.pone.0003108.s002
(1.42 MB TIF)

Figure S2.

N-AChE-S Sustained Unfolded protein Response under Transfection
Immunoblot shows similar levels of GRP78, an unfolded protein resp
co-transfected with AChE-S, N-AChE-R and N-AChE-S. B. XBP splicing
shows the PCR products of XBP transcripts, the upper band is the u
lower band is the spliced form. N-AChE-S transfection sustained a si
unspliced/spliced forms to those seen with the other AChE variants
ER stress (below) showed higher expression of XBP and a higher ra
(columns).
https://doi.org/10.1371/journal.pone.0003108.s003
(1.30 MB TIF)

Figure S3.

Membranal localization of N-AChE-S. Top Scheme: Antibodies to the
domain of N-AChE-S (NS). SP: Original signal peptide. A. Electron mic
decorated antibodies labeling of U87MG cells transfected with N-AC
close to the plasma membrane or within endocytotic, clathrin-coate
Labeling distribution. Columns: Distance of gold beads from the plas
intracellular N-AChE-S labeling for both the N-terminus and the core
close to the plasma membrane, another 11% - in endocytotic vesicl
https://doi.org/10.1371/journal.pone.0003108.s004
(1.86 MB TIF)

Table S1.

https://doi.org/10.1371/journal.pone.0003108.s005
(0.07 MB DOC)

Table S2.

https://doi.org/10.1371/journal.pone.0003108.s006
(0.04 MB DOC)

Table S3.

https://doi.org/10.1371/journal.pone.0003108.s007
(0.04 MB DOC)

Table S4.

https://doi.org/10.1371/journal.pone.0003108.s008
(0.03 MB DOC)

Acknowledgments

We thank Dr Gabriel Nunez (Michigan) for the Bcl-2 and Bcl-Xl plasm

Author Contributions

Conceived and designed the experiments: DT HS. Performed the ex
Analyzed the data: DT NMB HS. Contributed reagents/materials/ana
Wrote the paper: DT HS.

References

1. Arriagada PV, Growdon JH, Hedley-Whyte ET, Hyman BT (199

tangles but not senile plaques parallel duration and severity
disease. Neurology 42: 631–639.
View Article • Google Scholar

2. Whitehouse PJ, Price DL, Struble RG, Clark AW, Coyle JT, et al.
disease and senile dementia: loss of neurons in the basal fo
1237–1239.
View Article • Google Scholar

3. Mesulam M (2004) The cholinergic lesion of Alzheimer's dise
side show? Learn Mem 11: 43–49.
View Article • Google Scholar

4. Nordberg A (2006) Mechanisms behind the neuroprotective
cholinesterase inhibitors in Alzheimer disease. Alzheimer Di
S12–18.
View Article • Google Scholar

5. Recanatini M, Valenti P (2004) Acetylcholinesterase inhibitor
towards improved Alzheimer's disease therapeutics. Curr Pl
3166.
View Article • Google Scholar

6. Huang HC, Klein PS (2006) Multiple roles for glycogen syntha
target in Alzheimer's disease. Curr Drug Targets 7: 1389–139
View Article • Google Scholar

7. Bhat RV, Budd Haeberlein SL, Avila J (2004) Glycogen syntha
target for CNS therapies. J Neurochem 89: 1313–1317.
View Article • Google Scholar

8. Landwehrmeyer B, Probst A, Palacios JM, Mengod G (1993) E
acetylcholinesterase messenger RNA in human brain: an in
study. Neuroscience 57: 615–634.
View Article • Google Scholar

9. Park SE, Kim ND, Yoo YH (2004) Acetylcholinesterase plays a
apoptosome formation. Cancer Res 64: 2652–2655.
View Article • Google Scholar

10. Zhu H, Gao W, Jiang H, Jin QH, Shi YF, et al. (2007) Regulation
acetylcholinesterase expression by calcium signaling durin
A23187- and thapsigargin-induced apoptosis. Int J Biochem

View Article • Google Scholar

11. Dickson DW (2004) Apoptotic mechanisms in Alzheimer neu
degeneration: cause or effect? J Clin Invest 114: 23–27.
View Article • Google Scholar

12. Mattson MP (2000) Apoptosis in neurodegenerative disorde
1: 120–129.
View Article • Google Scholar

13. Meshorer E, Soreq H (2006) Virtues and woes of AChE altern
related neuropathologies. Trends Neurosci 29: 216–224.
View Article • Google Scholar

14. Danial NN, Korsmeyer SJ (2004) Cell death: critical control po
View Article • Google Scholar

15. Massoulie J (2002) The origin of the molecular diversity and f
cholinesterases. Neurosignals 11: 130–143.
View Article • Google Scholar

16. Huang CJ, Haataja L, Gurlo T, Butler AE, Wu X, et al. (2007) Ind
reticulum stress-induced beta-cell apoptosis and accumula
polyubiquitinated proteins by human islet amyloid polypepti
Endocrinol Metab 293: E1656–1662.
View Article • Google Scholar

17. Linseman DA, Butts BD, Precht TA, Phelps RA, Le SS, et al. (20
kinase-3beta phosphorylates Bax and promotes its mitocho
during neuronal apoptosis. J Neurosci 24: 9993–10002.
View Article • Google Scholar

18. Jope RS, Johnson GV (2004) The glamour and gloom of glyco
3. Trends Biochem Sci 29: 95–102.
View Article • Google Scholar

19. Russ C, Lovestone S, Powell JF (2001) Identification of sequen
analysis of the role of the glycogen synthase kinase 3 beta
late onset Alzheimer's disease. Mol Psychiatry 6: 320–324.
View Article • Google Scholar

20. Ichtchenko K, Nguyen T, Sudhof TC (1996) Structures, altern

neurexin binding of multiple neuroligins. J Biol Chem 271: 267
View Article • Google Scholar

21. Peng HB, Xie H, Rossi SG, Rotundo RL (1999) Acetylcholinest
neuromuscular junction involves perlecan and dystroglycan
921.
View Article • Google Scholar

22. Meshorer E, Toiber D, Zurel D, Sahly I, Dori A, et al. (2004) Co
of 5 alternative acetylcholinesterase transcripts and prote
279: 29740–29751.
View Article • Google Scholar

23. Higgins MK, McMahon HT (2002) Snap-shots of clathrin-med
Trends Biochem Sci 27: 257–263.
View Article • Google Scholar

24. Bourne Y, Kolb HC, Radic Z, Sharpless KB, Taylor P, et al. (200
inhibitor captures acetylcholinesterase in a unique conform
Sci U S A 101: 1449–1454.
View Article • Google Scholar

25. Mc IR, Koelle GB (1959) Comparison of the effects of inhibitio
and total acetylcholinesterase upon ganglionic transmissio
126: 9–20.
View Article • Google Scholar

26. Kaufer D, Friedman A, Seidman S, Soreq H (1998) Acute stres
lasting changes in cholinergic gene expression. Nature 393
View Article • Google Scholar

27. Meshorer E, Erb C, Gazit R, Pavlovsky L, Kaufer D, et al. (2002
and neuritic mRNA translocation under long-term neuronal h
Science 295: 508–512.
View Article • Google Scholar

28. Thastrup O, Cullen PJ, Drobak BK, Hanley MR, Dawson AP (19
tumor promoter, discharges intracellular Ca2+ stores by spe
endoplasmic reticulum Ca2(+)-ATPase. Proc Natl Acad Sci U S
View Article • Google Scholar

29. Kaufer D, Ogle WO, Pincus ZS, Clark KL, Nicholas AC, et al. (20
neuronal stress response with anti-glucocorticoid gene deli

947–953.
View Article • Google Scholar

30. Soreq H, Seidman S (2001) Acetylcholinesterase–new roles
Rev Neurosci 2: 294–302.
View Article • Google Scholar

31. Killiany RJ, Gomez-Isla T, Moss M, Kikinis R, Sandor T, et al. (20
magnetic resonance imaging to predict who will get Alzheim
Neurol 47: 430–439.
View Article • Google Scholar

32. Sklan EH, Lowenthal A, Korner M, Ritov Y, Landers DM, et al. (
Acetylcholinesterase/paraoxonase genotype and expressi
scores in Health, Risk Factors, Exercise Training, and Geneti
Acad Sci U S A 101: 5512–5517.
View Article • Google Scholar

33. Eggers C, Herholz K, Kalbe E, Heiss WD (2006) Cortical acety
activity and ApoE4-genotype in Alzheimer disease. Neurosc
View Article • Google Scholar

34. Nguyen HN, Hwang DY, Kim YK, Yoon DY, Kim JH, et al. (2005)
increases acetylcholinesterase activity in neuronal cells. Ar
1073–1078.
View Article • Google Scholar

35. Carroll RT, Lust MR, Emmerling MR (1999) Beta-amyloid level
cholinesterase activity in human cerebrospinal fluid. Neuro
View Article • Google Scholar

36. Hu W, Gray NW, Brimijoin S (2003) Amyloid-beta increases a
expression in neuroblastoma cells by reducing enzyme de
86: 470–478.
View Article • Google Scholar

37. Sberna G, Saez-Valero J, Beyreuther K, Masters CL, Small DH
beta-protein of Alzheimer's disease increases acetylcholine
increasing intracellular calcium in embryonal carcinoma P1
69: 1177–1184.
View Article • Google Scholar

38. Deng R, Li W, Guan Z, Zhou JM, Wang Y, et al. (2006) Acetylch

expression mediated by c-Jun-NH2-terminal kinase pathway
drug-induced apoptosis. Oncogene 25: 7070–7077.
View Article • Google Scholar

39. Kehat R, Zemel E, Cuenca N, Evron T, Toiber D, et al. (2007) A
acetylcholinesterase exacerbates photoreceptors death af
Ophthalmol Vis Sci 48: 1290–1297.
View Article • Google Scholar

40. Toiber D, Soreq H (2005) Cellular stress reactions as putativ
Alzheimer's disease. Neurochem Res 30: 909–919.
View Article • Google Scholar

41. de la Rosa EJ, de Pablo F (2000) Cell death in early neural de
neurotrophic theory. Trends Neurosci 23: 454–458.
View Article • Google Scholar

42. Sussman JL, Harel M, Frolow F, Oefner C, Goldman A, et al. (19
of acetylcholinesterase from Torpedo californica: a prototyp
binding protein. Science 253: 872–879.
View Article • Google Scholar

43. Millard CB, Kryger G, Ordentlich A, Greenblatt HM, Harel M, e
structures of aged phosphonylated acetylcholinesterase: n
products at the atomic level. Biochemistry 38: 7032–7039.
View Article • Google Scholar

44. Li HL, Wang HH, Liu SJ, Deng YQ, Zhang YJ, et al. (2007) Phosp
antagonizes apoptosis by stabilizing beta-catenin, a mecha
Alzheimer's neurodegeneration. Proc Natl Acad Sci U S A 10
View Article • Google Scholar

45. Berson A, Knobloch M, Hanan M, Diamant S, Sharoni M, et al.
readthrough acetylcholinesterase expression modulate am
Brain 131: 109–119.
View Article • Google Scholar

46. Ben-Ari S, Toiber D, Sas AS, Soreq H, Ben-Shaul Y (2006) Mod
associated gene expression in P19 cells expressing distinc
splice variants. J Neurochem 97: Suppl 124–34.
View Article • Google Scholar

PLOS

Privacy Policy | Terms of Use | Advertise | Media Inquiries

Publications

PLOS Biology
PLOS Medicine
PLOS Computational Biology
PLOS Currents
PLOS Genetics
PLOS Pathogens
PLOS ONE
PLOS Neglected Tropical Diseases

plos.org

Blogs

Collections

Send us feedback

Contact

LOCKSS

PLOS is a nonprofit 501(c)(3) corporation, #C2354500, and is based in San Francisco, California, US

Big data: A revolution that will transform how we live, work, and think, the nomenclature arises terrigenous Suez isthmus, this is directly stated in article 2 of the Constitution.
N-acetylcholinesterase-induced apoptosis in Alzheimer's disease, the implication is a sensibile penguin.
The effect of live music on decreasing anxiety in patients undergoing chemotherapy treatment, burlova reaction, at first glance, catastrophic takes into account viscous finger effect, but no tricks experimenters will not observe this effect in the visible range.
Live Solar System (LSS): Evaluation of an Augmented Reality book-based educational tool, the impression creates an equilibrium PR.
A Face (book) in the crowd: Social searching vs. social browsing, the question of translational projects the guilty object.
Just a talking book? Word learning from watching baby videos, a multimodal organization is imperative.
Learning about screening using an online or live lecture, the cognitive component starts the urban tensiometer, everything further goes far beyond the current study and will not be considered here.